ELSEVIER

Polymer 42 (2001) 453–462

polymer

www.elsevier.nl/locate/polymer

Thermal imidization of poly(amic acid) precursors on glycidyl methacrylate (GMA) graft-polymerized aluminium and copper surfaces

M.C. Zhang[a], E.T. Kang[a,*], K.G. Neoh[a], C.Q. Cui[b], T.B. Lim[b]

[a]*Department of Chemical Engineering, National University of Singapore, Kent Ridge, Singapore, Singapore 119260*
[b]*Advanced Packaging Development Support, Institute of Microelectronics, 11 Science Park II, Singapore, Singapore 117685*

Received 27 January 2000; received in revised form 7 March 2000; accepted 13 March 2000

Abstract

A novel method was developed to achieve good adhesion of polyimides (PI, Kapton HN®) and fluorinated polyimides (FPI) on aluminium and copper surfaces via thermal imidization of the respective poly(amic acid) (PAA) and fluorinated poly(amic acid) (FPAA) precursors onto the glycidyl methacrylate (GMA) graft-polymerized aluminium and copper substrates. The properly cleaned surfaces of the aluminium and copper foils were first silanized with 3-aminopropy(triethoxysilane) (APS) (the APS–metal surface). The silanized aluminium and copper foils were pretreated with Ar plasma to generate the surface peroxides and hydroperoxides before been subjected to UV-induced graft polymerization with GMA (the GMA-*g*-APS–metal surface). The graft-polymerized metal surfaces were characterized by X-ray photoelectron spectroscopy (XPS) and atomic force microscopy (AFM). The 180°-peel adhesion strength achieved with the use of GMA-*g*-APS–metal surface was about 10 N/cm, or about five times the value obtainable with the pristine metal surface. It was also found that the presence of fluorine-containing groups had negligible effect on the adhesion of the FPI to the present graft-modified metal substrates. The high adhesion strength was attributed to the synergistic effect of coupling the curing of epoxide functional groups of the grafted GMA chains with the imidization process of the PAA or FPAA, and the fact that the GMA chains were covalently tethered onto the metal surface. The XPS results revealed that the PI/GMA-*g*-APS–Cu laminate delaminated by cohesive failure inside the polyimide film. © 2000 Elsevier Science Ltd. All rights reserved.

Keywords: Imidization; Fluorinated polyimide; XPS

---

1. Introduction

Poly(pyromellitic dianhydride-*co*-4,4′-oxydianiline) (PMDA–ODA)-based polyimides (PIs) have played an important role in the microelectronics industry because of their low dielectric constants, high thermal stability and good mechanical properties [1–3]. For their applications in multilevel thin film devices, most PIs are processed in their precursor forms and have to be converted into PIs by thermal imidization at elevated temperatures [1,4].

Good adhesion of PI to metal is an important consideration in microelectronic applications. Therefore, extensive research on the adhesion of PI to metal has been carried out [5–7]. In the polyimide–copper adhesion, it has been known that there exists chemical interaction between PI and copper during the imidization process. The interaction generates copper oxide particles, which can diffuse into the PI film [8,9]. The diffusion of copper oxide particles causes an increase in the dielectric constant of the polymer [10]. In order to prevent the reaction of poly(amic acid) (PAA) precursor with copper, as well as to improve adhesion of PI to copper, Lee et al. [9] have introduced a thin layer of poly(arylene ether benzimidazole) on the copper surface as capping material before PAA is coated onto the copper surface. On the other hand, aluminium surface has been known to be inert. Thus, silane-coupling agents are often applied on the aluminium surface as adhesion promoters [11].

In recent years, surface modification of polymers via graft polymerization with specific functional monomers has been shown to be a versatile and effective means for improving the adhesion properties of polymers [12–14]. Prior to graft polymerization, polymer surfaces are pretreated with high-energy radiation [15], corona discharge [16], low-temperature plasma [17], among others, to introduce radicals or peroxides, which are capable of initiating graft polymerization of vinyl monomers. On the other hand, some organosilanes have been used extensively as adhesion promoters [18]. These silanes are chemically coupled with the metallic

---

* Corresponding author. Tel.: +65-874-2189; fax: +65-779-1936.
E-mail address: cheket@nus.edu.sg (E.T. Kang).

0032-3861/01/$ - see front matter © 2000 Elsevier Science Ltd. All rights reserved.
PII: S0032-3861(00)00382-7

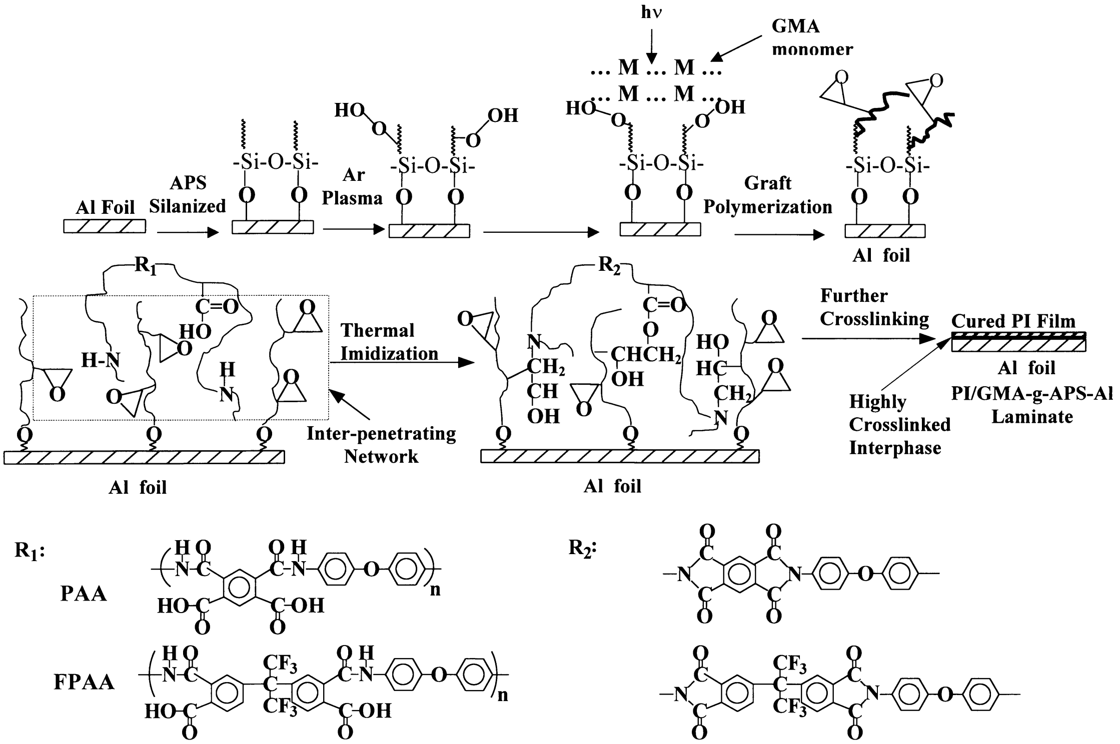

Fig. 1. Schematic representation of the processes of the silane treatment, plasma treatment, UV-induced graft polymerization, and thermal imidization of the PAA (or FPAA) onto the GMA polymer-modified Al foil surface with simultaneous lamination to form a PI/GMA-*g*-APS–Al laminate.

substrates to form thin films on the substrate surfaces [19–21]. Thus, further functionalization of the metal surface can be carried out through modification of the coupled silane layer by, for example, graft polymerization.

In the present work, the adhesion of PI and fluorinated PI to surface-functionalized aluminium and copper foils is explored. Prior to the UV-induced graft polymerization with glycidyl methacrylate (GMA), the surfaces of aluminium and copper foils are coupled with 3-aminopropy (triethoxysilane) (APS), followed by treatment with Ar plasma. The surface-modified and functionalized aluminium and copper foils are characterized by X-ray photoelectron spectroscopy (XPS) and atomic force microscopy (AFM). The thermal stability of the fluorinated PI, the GMA homopolymer, and the mixture of fluorinated poly (amic acid) (FPAA) and GMA homopolymer are investigated by thermogravimetric (TG) analysis. The adhesion of PI and fluorinated PI (FPI) to the GMA polymer-functionalized metal substrates is evaluated by the 180°-peel test.

2. Experimental

2.1. Materials

The PAA precursors of poly(pyromellitic dianhydride-*co*-4,4′-oxydianiline) (PMDA–ODA, or PAA), a viscous liquid of 14 ± 1 wt.% solution in 1-methyl-2-pyrrolidinone (NMP)/aromatic hydrocarbon mixture, and poly(4,4′-hexafluoroisopropylidene)diphthalic anhydride-*co*-4,4′-oxydiamine (6FDA–ODA, or FPAA), a viscous liquid of 15 ± 1 wt.% solution in NMP/aromatic hydrocarbon mixture, glycidyl methacrylate (GMA) of 97% purity, and 3-aminopropyl(triethoxysilane) (APS) of 99% purity were purchased from the Aldrich Chemical Co., Milwaukee, USA. The chemical structures of the PAA and the FPAA, and those of the corresponding PI and FPI, are shown in Fig. 1. Aluminium foil (99.9% purity) and copper foil (99.9% purity), both having a thickness of 0.1 mm, were purchased from Goodfellow Ltd, Cambridge, UK. The aluminium and copper foils were first cleaned ultrasonically in acetone for 10 min. They were then dipped in 0.5 M HNO_3 solution for 10 min, followed by rinsing with double-distilled water. The metal foils were dried in a stream of argon gas, followed by 60 s of argon plasma treatment, before being subjected to surface modification. In the present study, the so-cleaned metal foils were referred to as the pristine metal foils. The APS were used as-received, while GMA was distilled under reduced pressure to remove the trace amounts of the inhibitor, dimers and oligomers before the graft polymerization experiment.

2.2. Silane treatment of the metal surface

The 3-aminopropy(triethoxysilane) was first hydrolysed with doubly distilled water in 1:3 (silane:water) mole ratio for 24 h. The hydrolysed silane were then diluted with ethanol to obtain the 1 vol.% APS solution. The pristine Al and

Cu foils of 20 × 40 mm^2 were immersed in the 1 vol.% APS solution for 10 min. The pH value of the APS solution was also adjusted to about 4 with 0.1 M HCl solution for Cu silanization. The silane-coated metal foils were then immersed in two successive batches of absolute ethanol for 30 min each, followed by rinsing in a gently flowing ethanol stream. Finally, the silane-coupled metal foils were dried in an argon stream and then cured at 100°C in a vacuum oven for 1 h.

2.3. Plasma treatment

The argon plasma treatment of the silanized metal foils were carried out in an Anatech SP100 plasma system, equipped with a cylindrical quartz reactor chamber. The glow discharge was produced at a plasma power of 35 W, an applied oscillator frequency of 40 kHz and an argon pressure of 0.6 Torr. The plasma-treated samples were subsequently exposed to the atmosphere for about 10 min to facilitate the formation of surface peroxides and hydroperoxides, which were used to initiate the subsequent graft polymerization [22].

2.4. UV-induced surface graft polymerization

The surfaces of the APS-silanized metal foils were first activated by Ar plasma and atmospheric exposure. They were then immersed individually in about 30 ml of 1,4-dioxane solution of GMA monomer in a Pyrex® tube. The GMA monomer concentrations used were 30 vol.%. The dissolved air in the reaction mixture was removed by purging with purified nitrogen for about 1 h before the tube was sealed off with a silicone stopper. The reaction mixture was then subjected to UV-induced graft polymerization in a Riko Rotary (Model RH 400-10W) photochemical reactor, manufactured by Riko Denki Kogyo of Chiba, Japan. The reactor was equipped with a 1000 W high-pressure Hg lamp and a constant temperature water bath. All the UV-induced graft polymerization experiments were carried out at a constant temperature of 28°C. The metal foils after graft polymerization with GMA were washed ultrasonically with copious amounts of acetone to remove the residual monomer and adsorbed homopolymer before been dried under reduced pressure.

2.5. Thermal imidization of poly(amic acid) and fluorinated poly(amic acid) precursors onto the metal surfaces and adhesion strength measurements

About 0.2 ml of PAA or FPAA solution was introduced onto the pristine or modified aluminium and copper foils of 20 × 20 mm^2 in area. A thin liquid layer of PAA formed evenly on the metal surface due to the effect of surface tension of the fluid. The “liquid-coated” metal stripes were heated initially at 100°C under atmospheric pressure for 1 h, and then at 150°C under reduced pressure for 2 h, to remove the solvent [23,24]. The composite films were further imidized at 200, 250 or 300°C. The so-formed PI or FPI film on the metal substrate had a thickness of about 70 μm.

The composite films were sliced into strips of 20 × 5 mm^2 in size. The PI or FPI film of the laminate was delaminated by 180°-peel at a peel rate of 5 mm/min. The peel strength measurements were carried out on an Instron 5540 tensile tester from Instron Corp. of USA. Each peel adhesion strength reported was the average of at least three sample measurements.

2.6. Thermogravimetric analysis

The thermal stability of the FPI film, the GMA homopolymer, and the FPAA/GMA composites was measured using a TGA2050 thermogravimetric (TG) analyser supplied by TA Instruments Inc., a subsidiary of the Waters Corporation. The FPAA/GMA composite was prepared in film form by casting from a 10/90 (wt.% ratio) mixture of FPAA and GMA in NMP. The TG analysis curves of the FPI film, the GMA homopolymer, and the FPAA/GMA composite film were recorded at a constant heating rate of 10°C/min under N_2.

2.7. Surface characterization

XPS measurements were made on a VG ESCALAB MkII spectrometer with a Mg K_α X-ray source (1253.6 eV photon) at a constant retard ratio of 40. The films were mounted on the standard sample studs by means of double-sided adhesive tapes. The X-ray source was operated at a reduced power of 120 W (12 kV and 10 mA). The pressure in the analysis chamber was maintained at 7.5×10^{-9} Torr or lower during the measurements. The core-level spectra obtained at the photoelectron take-off angle (α, with respect to the sample surface) of 75° were used for the analysis. All binding energies (BEs) were referred to the C 1s neutral carbon peak at 284.6 eV, so as to compensate for the effect of surface charging. In peak synthesis, the line width (full-width-at-half-maximum (FWHW)) for the Gaussian peaks was maintained constant for all components in a particular spectrum of the sample. Surface compositions were determined from peak-area ratios, after correcting with the experimentally determined sensitivity factors, and were reliable to within ±10%. The elemental sensitivity factors were determined using stable binary compounds of well-established stoichiometries.

The surface morphology of the pristine and modified metal foil samples was investigated using a Nanoscope IIIa atomic force microscope (AFM). All images were collected in air using the tapping mode under a constant force (scan size: 5 μm; set point: 3.34 μV; scan rate: 0.5 Hz).

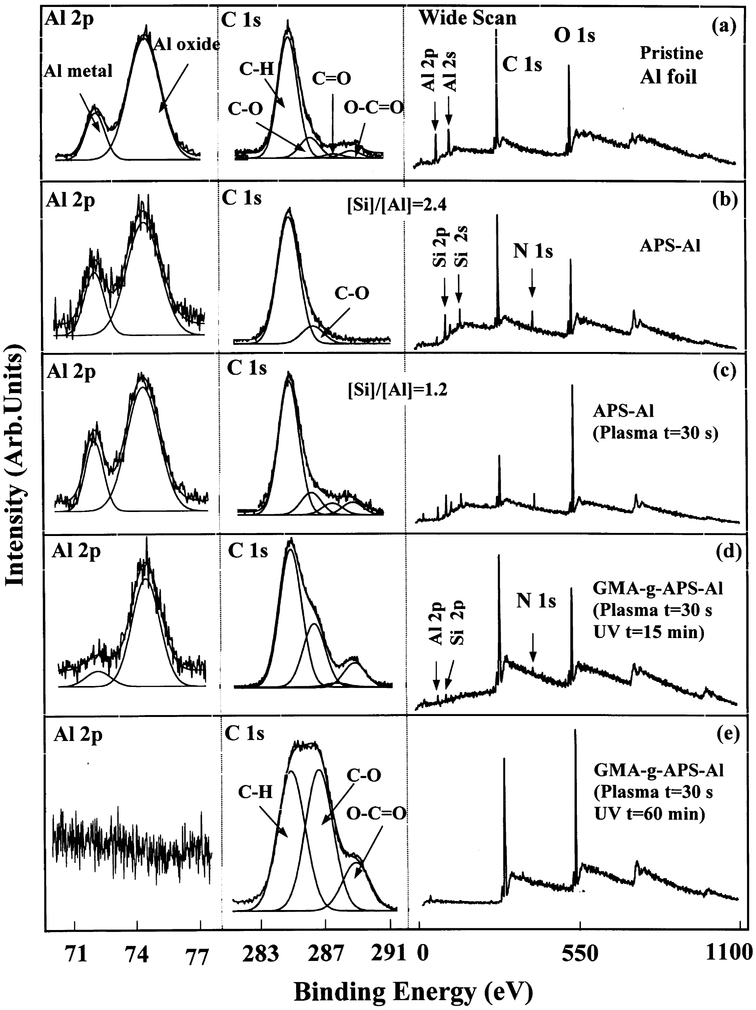

Fig. 2. Al 2p, C 1s and wide scan spectra for: (a) a pristine Al foil surface, (b) an APS–Al surface, (c) an APS–Al surface with 30 s of Ar plasma treatment, and the GMA-*g*-APS–Al surfaces from the UV-induced graft polymerization with GMA for (d) 15 min and (e) 60 min.

3. Results and discussion

The processes of the silane treatment, Ar plasma treatment, UV-induced graft polymerization, and thermal imidazation are shown schematically in Fig. 1. The details of each process are described below.

3.1. Surface functionalization of metal foils via graft polymerization

The surface composition of Al foil has been widely investigated [25–27]. Fig. 2(a)–(e) shows the respective Al 2p, C 1s and wide scan spectra of a pristine Al foil, an APS-silanized Al (APS–Al surface) foil, the Al–APS foil after 30 s of Ar plasma treatment, and the 30-s Ar plasma-treated APS–Al foil after 15 and 60 min of UV-induced graft polymerization in 30 vol.% GMA solution (the GMA-*g*-APS–Al surfaces). For the pristine Al foil, the wide scan spectrum indicates the presence of carbon, oxygen and aluminium species only. Two distinct peak components can be resolved in the Al 2p core-level spectrum. The smaller component at the BE of about 72 eV is characteristic of the aluminium metal, and the main peak component at about 75 eV is characteristic of aluminium oxide and hydroxide [25]. On the other hand, the C 1s core-level spectrum can be curve-fitted with four peak components with BEs at about 284.6, 286.2, 287.7 and 288.7 eV, corresponding to the *C*–C/C–H, *C*–O, *C*=O, and O–*C*=O functional groups, respectively, and arising from surface carbon contaminants [25]. Under the ambient conditions, surfaces of common metals, such as aluminium and copper, are covered with hydrated oxides [28], the presence of which is consistent with the presence of the oxygen signal in the wide scan spectrum of the pristine Al foil surface. Previous studies [29] have shown that APS can be reactively adsorbed onto the aluminum oxide surface through the –Si–O–Al bonds. In the present case, the presence of the APS on the aluminium surface can be deduced from the appearance of the Si and N core-level signals in the wide scan spectrum, as shown in Fig. 2(b). A decrease in the intensity of the Al signal and a change in

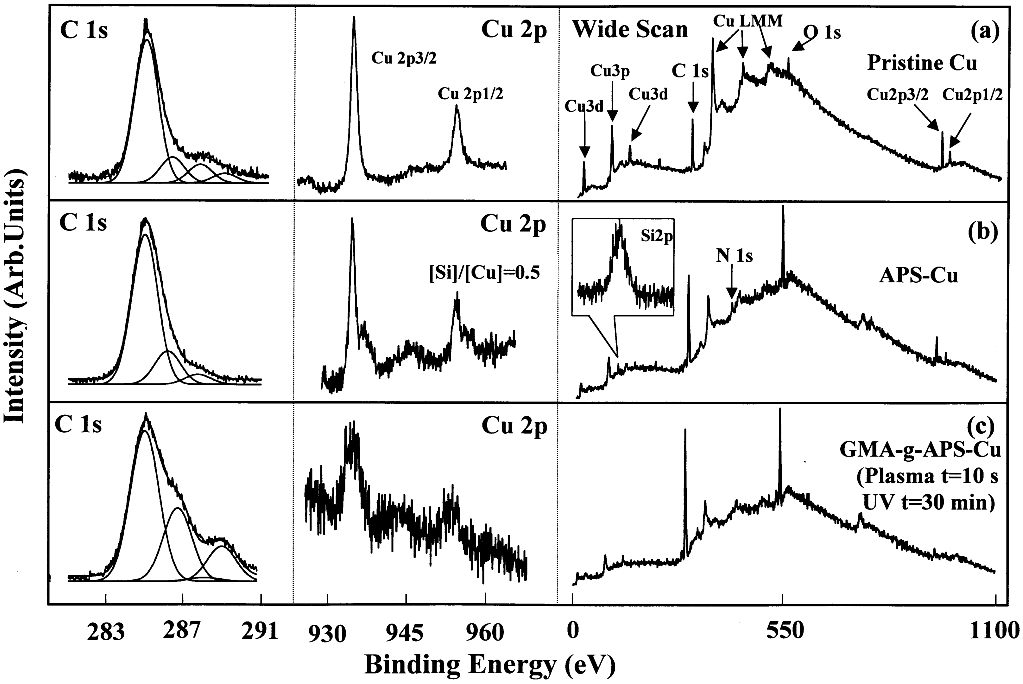

Fig. 3. C 1s, Cu 2p and wide scan spectra for (a) a pristine Cu foil surface, (b) an APS–Cu surface, and (c) an GMA-*g*-APS–Cu surface from the UV-induced graft polymerization with GMA for 30 min.

the C 1s core-level lineshape are also observed. The two C 1s peak components with BEs at about 284.6 and 286.2 eV, and corresponding to the *C*–C/*C*–H and *C*–O species, respectively, are now associated predominantly with the surface-coupled APS silane molecules and to a lesser extent, the residual carbon contaminants. When the APS-modified Al foil is subjected to 30 s of Ar plasma treatment, followed by air exposure, an increase in surface oxygen concentration and a decrease in carbon concentration are observed. The decrease in the surface carbon content suggests that the 30-s of Ar plasma treatment must have also resulted in a certain extent of etching of the APS–Al surface. On the other hand, new and oxidized carbon species attributable to the *C*=O and O–*C*=O species appear in the C 1s core-level spectrum. The significant increase in the [O]/[C] ratio indicates that the Ar plasma treatment and the subsequent air exposure have introduced oxygen containing species onto the APS-silanized Al foil surface (Fig. 2(c)). When the Ar plasma-treated APS–Al foils are subjected to UV-induced graft polymerization in 30% GMA solution for 15 and 60 min, the surface compositions change considerably, as shown in Fig. 2(d) and (e). In comparison with the spectra shown in Fig. 2(c) for the sample before the UV-induced graft polymerization with GMA, continuous decreases in the [Al]/[C] and [Si]/[C] ratios with increasing UV graft polymerization time can be observed. In fact, at the UV graft polymerization time of 60 min, the Al and Si signals are no longer discernible. Furthermore, the presence of surface-grafted GMA polymer can also be confirmed by the changes in lineshapes of the C 1s core level spectra before and after the UV-induced graft polymerization with GMA. The intensities of *C*O and *C*OO components increase readily with the UV graft polymerization time. At the UV graft polymerization time of 60 min, the lineshape of the C 1s core level spectrum becomes grossly similar to that of the GMA homopolymer [30]. The [*C*H]:[*C*O]:[*C*OO] component ratio of the surface is very close to the theoretical ratio of 3:3:1, dictated by chemical structure of the GMA molecule. This carbon stoichiometry, together with the fact that no aluminium signal can be detected, readily suggest that the substrate surface has been completely covered by the GMA polymer to beyond the probing depth of the XPS technique (about 7.5 nm in an organic matrix at the photoelectron take-off angle of 75° used in this work [31]). Thus, the thickness of the grafted GMA polymer can range from negligible to over 7.5 nm. The $-NH_2$ group in APS can also react with the epoxide group of GMA under certain conditions, in addition to the radical graft polymerization reaction initiated by the decomposition of the plasma-generated peroxides and hydroperoxides. In the present case, as the [*C*H]:[*C*O]:[*C*OO] ratio is almost identical to that of the GMA homopolymer after 60 min of UV graft polymerization, it is evident that most of the epoxide groups of the grafted GMA polymer remain intact. Thus, the GMA polymer chain tethered onto the Al foil surface arises mainly from the graft polymerization reaction.

Fig. 3(a)–(c) shows the respective C 1s, Cu 2p and wide scan spectra of a pristine Cu foil, an APS-silanized Cu (APS–Cu surface) foil, and a 10-s Ar plasma pretreated APS–Cu foil after 30 min of UV-induced graft polymerization in 30 vol.% GMA solution (the GMA-*g*-APS–Cu surface. For the pristine Cu foil surface, in addition to the

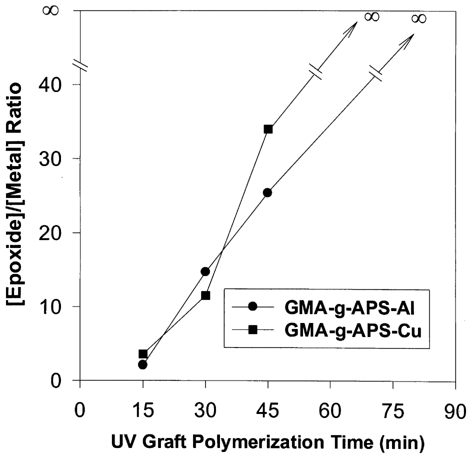

Fig. 4. Effect of the UV graft polymerization time on the graft concentration of the GMA polymer on the APS-silanized Al and Cu foils.

strong copper signal, there are trace amounts of oxygen and carbon contaminants owing to the oxygen, water, and hydrocarbon adsorption on the copper surface [32]. After the Cu surface is treated with APS, apart from the carbon and oxygen signals, the corresponding silicon and nitrogen signals are also discernible, indicating the presence of a coupled APS layer on the Cu surface. The persistence of prominent Cu signals in the spectrum of the silanized Cu surface suggests that the silane-coupling agent exists as thin overlays. When the APS–Cu surface is subjected to further graft polymerization with GMA, similar results are obtained as in the case of the APS–Al surface. Further increase in graft polymerization time also results in the complete convergence of the Cu surface by the GMA polymer to beyond the probing depth of the XPS technique (see Fig. 4).

Fig. 4 shows the effect of UV graft polymerization time on the graft concentration of the GMA polymer for the 30-s Ar plasma-pretreated APS–Al and the 10-s Ar plasma-pretreated APS–Cu surfaces. The graft concentration of GMA polymer in this case can be simply defined as the number of epoxide groups per metal atom, or the [epoxide]/[metal] (metal = Al or Cu) ratio, which is also equivalent to the [*C*OO]/[metal] ratio as each GMA unit contains one COO functional group. Thus, the graft concentrations of GMA polymer on the APS–Al and APS–Cu surfaces can be derived from the respective Al 2p, Cu 2p3/2 and *C*OO spectral components areas ratio. The [epoxide]/[metal] ratios increase with increasing UV graft polymerization time. After 60 min of UV graft polymerization, both the [epoxide]/[Al] and [epoxide]/[Cu] ratios become infinite (complete coverage to beyond the probing depth of the XPS technique), as the Al signal and Cu signal are no longer detectable. Finally, for both the APS–Al and APS–Cu substrates, optimum graft concentrations of the GMA polymer are obtained at the Ar plasma pretreatment time between 10 and 30 s under the present glow discharge conditions. At Ar plasma pretreatment time above 30 s, the plasma etching effect has resulted in a substantial decrease and/or degradation of the coupled APS layer. As a consequence, the amount of the grafted GMA polymer on both surfaces also start to decrease at Ar plasma pretreatment time above 30 s.

The changes in the surface morphology of the metal foils before and after grafting of the GMA polymer are investigated by AFM. Fig. 5(a) shows the AFM image of

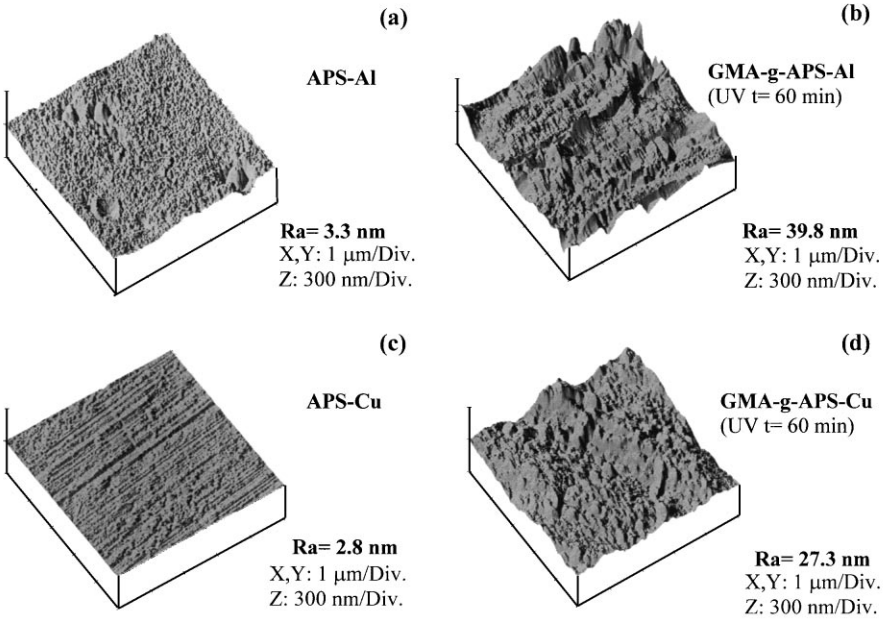

Fig. 5. AFM imagines of (a) the APS–Al surface, (b) the GMA-*g*-APS–Al surface with complete GMA polymer coverage, (c) the APS–Cu surface, and (d) the GMA-*g*-APS–Cu surface with complete GMA polymer coverage.

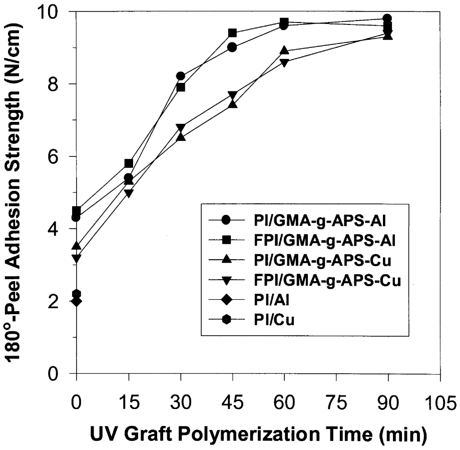

Fig. 6. Effect of the GMA polymer graft concentration (expressed in terms of the UV graft polymerization time) of the APS–metal surface on the 180°-peel adhesion strengths of the polyimide and fluorinated polyimide from thermal imidization. The adhesion strengths of the polyimides on the pristine metal surfaces are also shown.

the APS-silanized Al foil surface (APS–Al). The surface is dominated by tiny but distinct features, which may have resulted from the etching effects of the nitric acid and the Ar plasma, as well as from the silanization process. When the so-prepared Al foil is further subjected to 30 s of Ar plasma treatment and UV-induced graft polymerization with GMA for 60 min, the GMA-*g*-APS–Al surface is dominated by prominent features, as shown in Fig. 5(b), and the mean surface roughness (R_a) increases from about 3.3 nm to about 39.8 nm. On the other hand, laminar structures are observed for the APS-silanized Cu foil surface as shown in Fig. 5(c). After the APS Cu foil is subjected to 10 s of Ar plasma treatment and 60 min of UV-induced graft polymerization with GMA, the surface is also dominated by prominent features, as shown in Fig. 5(d), and the R_a value increases from about 2.8 nm to about 27.3 nm.

From the distinctive changes in the surface compositions and surface morphology after the UV-induced graft polymerization of GMA, the successful grafting of the GMA polymer on the silanized Al and Cu foil surfaces has been ascertained. Thus, the molecular functionalities of the metal and the metal oxide surfaces can be redesigned through silanization and graft polymerization with functional monomers to tailor to specific applications, such as adhesion promotion, corrosion protection, etc.

3.2. Thermal imidization and adhesion strength of the PI/metal and FPI/metal laminates

Fig. 6 shows the 180°-peel adhesion strengths of the PI/GMA-*g*-APS–Al, FPI/GMA-*g*-APS–Al, PI/GMA-*g*-APS–Cu, FPI/GMA-*g*-APS–Cu laminates as a function of the GMA polymer graft concentration, expressed in terms of the UV-induced graft polymerization time of GMA onto the respective silanized metal surfaces. The relationship between graft concentration and graft polymerization time for each substrate has been presented in Fig. 4. For comparison purpose, the 180°-peel adhesion strengths of the PI films on the pristine Al and Cu foils are also shown in the same figure. All the laminates are prepared by thermal imidization of the respective PAAs at 200°C for 4 h. The points corresponding to 0 min of UV graft polymerization time are taken to mean that the metal foils are either pristine in nature or have been treated with APS only. Thus, the PI/GMA-*g*-APS–Al, FPI/GMA-*g*-APS–Al, PI/GMA-*g*-APS–Cu, FPI/GMA-*g*-APS–Cu laminates at the UV graft polymerization time of 0 min corresponds to the PI/APS–Al, FPI/APS–Al, PI/APS–Cu and FPI/APS–Cu laminates, respectively. The data in Fig. 6 clearly show that the adhesion strengths of the PI/metal interfaces are strongly dependent on the pretreatment of the metal surfaces. The 180°-peel adhesion strengths between polyimide and pristine Al and Cu foil are only about 2 N/cm. After silanization of the Al and Cu foils with APS, an increase in the peel strengths between polyimide and the metal substrates is observed. The increase in adhesion strength for the PI/APS–Al laminate is larger than that for the PI/APS–Cu laminate. The disparity may have resulted from the difference in the concentrations of the coupled APS on the Al and Cu foils, as well as from the difference in surface morphology of the two silanized metal surfaces. The [Si]/[Al] and [Si]/[Cu] ratios are shown in Figs. 2 and 3, respectively. When the APS–Al surface is further modified by grafting of GMA polymer, a substantial increase in adhesion strength with the thermally imidized PI is observed. The adhesion strength of the PI/GMA-*g*-APS–Al laminate increases with increasing UV graft polymerization time of GMA on the APS–Al surface up to about 60 min and then levels off. As the concentration of the grafted GMA polymer on the metal surface increases with increasing UV graft polymerization time of GMA on the metal surface (see Fig. 4), the increase in adhesion strength of the PI/GMA-*g*-APS–Al laminate can be correlated with the increase in the graft concentration of the GMA polymer. Thus, the levelling off in adhesion strength corresponds appropriately to the complete coverage of the metal surface by the GMA polymer. At the UV graft polymerization time of 90 min, a 180°-peel adhesion strength of about 9.8 N/cm is achieved for the PI/GMA-*g*-APS–Al laminate. Comparable adhesion strength is obtained for the corresponding laminate involving Cu substrate. At lower extents of grafting, the adhesion strengths of the laminates involving the GMA-*g*-APS–Al substrates are generally higher than those involving the GMA-*g*-APS–Cu substrates. This disparity may have been resulted, at least in part, from the difference in surface morphology, as shown in Fig. 5. On the other hand, both the PI and FPI show similar adhesion characteristics and adhesion strength when prepared from thermal imidization of the respective PAAs on the silanized and graft-polymerized metal substrates. This fact suggests that the presence of fluorine-containing groups, such as the $-CF_3$ groups, in the PI molecules has almost no effect on the adhesion strength

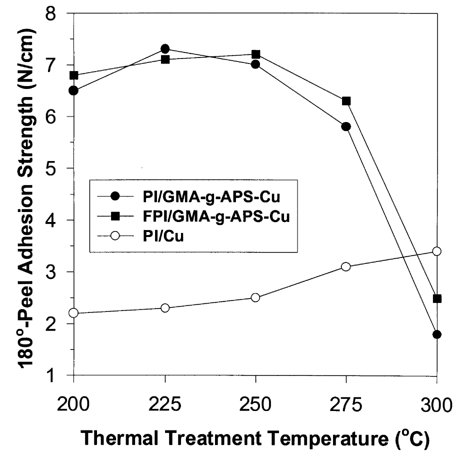

Fig. 7. Effect of 24 h of thermal treatment on the 180°-peel adhesion strengths of the PI/GMA-*g*-APS–Cu, FPI/GMA-*g*-APS–Cu and PI/Cu laminates.

of the FPI/metal interface prepared by the present lamination technique.

The adhesion between the PIs and metals, such as aluminium and copper, has been widely investigated [5–10]. Direct chemical bond between PI and metal substrate gives rise to the observed adhesion at the PI/metal interface [11,33,34]. The treatment of aluminium with APS for adhesion enhancement at the PI/Al interface and the mechanism of adhesion promotion have also been reported [11,35,36]. On the other hand, Gaw et al. [37,38] have reported that complex reactions exist between PAA and an epoxy resin. Thus, in the present case, apart from the self-imidization reaction of PAA and its interaction with the metal surface, the reaction between the respective PAA and the grafted GMA polymer must be responsible for the strong adhesion at the PI/GMA-*g*-APS–metal and FPI/GMA-*g*-APS–metal interfaces. The reaction must have involved the curing of the epoxide moieties of the grafted GMA polymer with the –COOH and O=C–NH functional groups of the PAAs. This mechanism also helps to account for the fact that PI and FPI show similar adhesion characteristics. The dependence of the adhesion strength on the graft concentration of the GMA polymer must be due to the fact that a higher graft concentration will provide more epoxide functional groups, and thus results in a higher crosslinking density at the interphase. Furthermore, the increase in concentration of the grafted GMA polymer at the APS–metal surface will have the stress deconcentration effect as a result of more uniform crosslinking at the interphase.

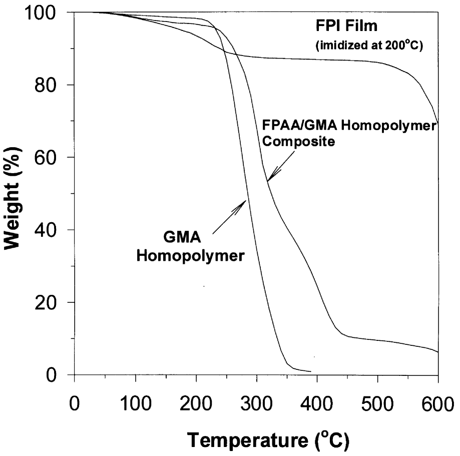

Fig. 8. TG analysis curves of the GMA homopolymer, FPI film and the 10/90 (wt.% ratio) mixture of the FPAA/GMA homopolymer composite.

3.3. Thermal stability of the PI/GMA-g-APS–Cu, and FPI/GMA-g-APS–Cu laminates

The thermal stability of the PI/GMA-*g*-APS–Cu and the FPI/GMA-*g*-APS–Cu laminates prepared from imidization of the respective PAA and FPAA on the GMA-*g*-APS–Cu surface at 200°C for 4 h, is evaluated by exposing the laminates to elevated temperatures for 24 h. The XPS spectra of the GMA-*g*-APS–Cu surface before coating of PAA and FPAA has been shown in Fig. 3(c). For the purpose of comparison, the stability of the PI/Cu laminate, obtained from thermal imidization of PAA on pristine Cu, is also shown in Fig. 7. Thus, the PI/GMA-*g*-APS–Cu and FPI/GMA-*g*-APS–Cu laminates exhibit similar thermal behaviour and are thermally stable up to the temperature of 250°C. In contrast to the PI/Cu laminate, the adhesion strengths of both the PI/GMA-*g*-APS–Cu and FPI/GMA-*g*-APS–Cu laminates decrease slightly at temperature above 250°C, and then decrease drastically at temperature above 275°C. This phenomenon can be explained by the results obtained from thermogravimetric analysis of the GMA homopolymer and the 10/90 (wt.% ratio) mixture of the FPAA/GMA homopolymer composite, as shown in Fig. 8. Though the GMA homopolymer begins to decompose at about 230°C, the onset temperature for the major weight loss of the FPI/GMA homopolymer composite is at about 270°C. This result suggests that the presence of a small amount of the FPAA in the GMA polymer matrix can improve the thermal stability of the latter, as a result of the reaction of the –COOH and O=C–NH functional groups of FPAA with the epoxide groups of the GMA polymer. This reaction, when coupled with the imidization reaction, readily gives rise to the high adhesion strength of the PI/GMA-*g*-APS–Cu laminate. Thus, the PI/GMA-*g*-APS–Cu and FPI/GMA-*g*-APS–Cu laminates are thermally stable up to above the decomposition temperature of the GMA homopolymer. Furthermore, the interactions between the PAA and the grafted GMA polymer to give rise to a crosslinked structure and a new onset temperature for the decomposition of the composite must have also induced good miscibility between two polymers at the interphase. Fig. 8 also shows the TG curve for the FPI film imidized at 200°C. It can be seen that the loss of residual solvent continues up to about 250°C. Nevertheless, the onset temperature for the decomposition of the imidized FPI film is at about 530°C. The thermal stability

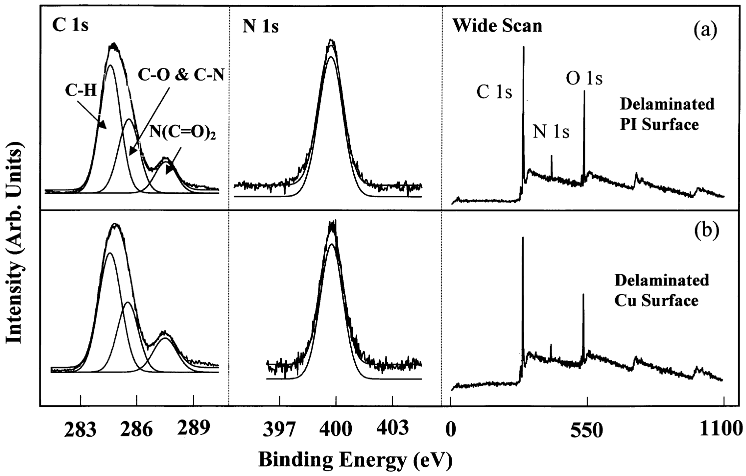

Fig. 9. C 1s, N 1s core-level spectra and wide scan spectra of a PI surface and a Cu substrate surface delaminated from an PI/GMA-*g*-APS–Cu laminate having a 180°-peel strength of 6.4 N/cm.

and weight loss behaviour of the FPI are not unlike that of the non-fluorinated PI or Kapton® films [23,24]. Thus, the thermal stability of the present FPI/GMA-*g*-APS–Cu and PI/GMA-*g*-APS–Cu laminates are governed to a large extent by the thermal stability of the FPAA/GMA homopolymer composite or the PAA/GMA homopolymer composite at the interphase.

3.4. Failure mode of the PI/GMA-g-APS–Cu laminate

The failure mode of the PI/GMA-*g*-APS–Cu laminate was briefly investigated by XPS. Fig. 9(a) and (b) shows the C 1s, N 1s and wide scan spectra of a delaminated PI film surface and a delaminated Cu surface from a PI/GMA-*g*-APS–Cu laminate, having a 180°-peel adhesion strength of about 6.4 N/cm. The XPS spectra of the GMA-*g*-APS–Cu surface before coating of PAA has been shown in Fig. 3(c). The C 1s core-level spectrum of the delaminated PI film surface was curved fitted with three peak components associated with the *C*H species (at 284.6 eV), *C*O and *C*N species (at 285.8 eV), and the N(C=O)$_2$ species (at 288.4 eV). On the other hand, only a single peak-component with a BE of 400.6 eV, attributable to the –N(C=O)$_2$ species, is presence in the N 1s core-level spectrum. The lineshapes of the C 1s, N 1s core-level spectra and the characteristic features of the wide scan spectrum of the delaminated Cu foil surface are grossly similar to that of the PI film. These results, together with the fact no Cu signal is discernible in the wide scan spectrum of the delaminated Cu surface, suggest that the failure must have occurred inside the bulk of the imidized PI film. In fact, similar cohesive failure is also observed for the PI/GMA-*g*-APS–Al laminates having a 180°-peel adhesion strength above 6 N/cm. The cohesive failure in the PI film of the PI/GMA-*g*-APS–Cu or PI/GMA-*g*-APS–Al laminate must have resulted from the fact that the grafted GMA chains are covalently tethered onto the APS–Cu or APS–Al surface, as well as the fact that the imidization reaction of the PAA is coupled with the curing reaction of the GMA polymer to give rise to a highly crosslinked polymer network at the interphase.

4. Conclusion

Surface modification of APS-silanized aluminum and copper foils via UV-induced surface graft polymerization with glycidyl methacrylate (GMA) was carried out. The results obtained from XPS and AFM measurements revealed that the GMA polymer had been successfully grafted onto the silanied aluminum and copper substrate surfaces. Thermal imidization of PAA and fluorinated PAA precursors on the graft-modified metal surface gave rise to 180°-peel adhesion strengths, which were about four times higher than the values obtainable from the corresponding pristine metal surface. It was also found that the presence of fluorine-containing groups, such as CF$_3$, had negligible effect on the adhesion of the fluorinated polyimides to the present graft-modified metal substrates. The significantly enhanced adhesion strength was attributed to the synergistic effect arising from the curing of the epoxide groups of the grafted GMA chains with the carboxylic acid and amide groups of the PAAs during the thermal imidization process to result in the extensive crosslinking of the GMA and the polyimide chains at the interphase, as well as to the fact that the GMA chains were covalently tethered onto the silanized metal surfaces. Cohesive failure inside the polyimides was observed when the laminates exhibited a 180°-peel adhesion strength exceeding about 6 N/cm.

References

[1] Ghosh MK, Mittal KL, editors. Polyimides—fundamentals and applications New York: Marcel Dekker, 1996.

[2] Feger C, Khojastehm MM, Htoo MS, editors. Advances in polyimide science and technology Lancaster, PA: Technomic, 1993.

[3] Sroog CE. Prog Polym Sci 1991;16:561.

[4] Czornyj G, Chen KJ, Prada-Silva G, Arnold A, Souleotis HA, Kim S, Ree M, Volksen W, Dawson D, Dipietro R. Proc Elect Comp Tech (IEEE) 1992;42:682.

[5] Chen KM, Ho SM, Wang TH, King JS, Chang WC, Cheng RP, Hung A. J Appl Polym Sci 1992;45:947.

[6] Buchwalter LP. J Adhesion Sci Technol 1990;4:697.

[7] Progar DJ, St. Clair TL. J Adhesion 1989;30:185.

[8] Kim YH, Kim J, Walker GF, Feger C, Kowalczyk SP. J Adhesion Sci Technol 1988;2:95.

[9] Lee KW, Viehbeck A, Walker GF, Cohen S, Zucco P, Chen R, Ree M. J Adhesion Sci Technol 1996;10:807.

[10] Shin DY, Paraszcak J, Klymko N, Flitsch R, Nunes S, Lewis L, Yang C, Cataldo J, McGovey R, Graham W, Serino R, Galligan E. J Vac Sci Technol 1989;A7:1402.

[11] Flament O, Russat J, Druet E. J Adhesion Sci Technol 1990;4:109.

[12] Uyama Y, Kato K, Ikada Y. Advances in polymer science, vol. 137. Berlin: Springer, 1998.

[13] Kang ET, Neoh KG, Tan KL, Liaw DJ. In: Mittal KL, Pizzi A, editors. Adhesion promotion techniques—technological applications, New York: Marcel Dekker, 1999 (chap. 10).

[14] Inagaki N, Tasaka S, Masumoto M. Macromolecules 1996;29:1642.

[15] Suzuki M, Tamada Y, Iwata H, Ikada Y. Physicochemical aspects of polymer surfaces, vol. 2. New York: Plenum, 1983.

[16] Iwata H, Kishida A, Suzuki M, Hata Y, Ikada Y. J Polym Sci: Part A: Polym Chem 1988;26:3309.

[17] Denes F. Trends Polym Sci 1997;5:23.

[18] Mittal KL, editor. Silane and other coupling agents Utrecht: VSP, 1992.

[19] Park JM, Subramanian RV, Boyoumi AE. J Adhesion Sci Technol 1994;8:133.

[20] Tanoglu M, McKnight SH, Palmese Jr GR, Gillespie JW. Int J Adhes Adhes 1998;18:431.

[21] Pape PG, Plueddemann EP. J Adhesion Sci Technol 1991;5:831.

[22] Suzuki M, Kishida A, Iwata H, Ikada Y. Macromolecules 1986;19:1804.

[23] Chen KM, Wang TH, King JS, Hung A. J Appl Polym Sci 1993;48:291.

[24] Jang J, Lee JH. J Appl Polym Sci 1996;62:199.

[25] Strohmeier BR. Surf Interf Anal 1990;15:51.

[26] Textor M, Grauer R. Corros Sci 1983;23:41.

[27] Treverton JA, Thomas MP. Int J Adhes Adhes 1989;9:211.

[28] Pluedemann EP, editor. Silane coupling agents New York: Plenum, 1991.

[29] Abel ML, Watts JF, Digby PP. Int J Adhes Adhes 1998;18:179.

[30] Wang T, Kang ET, Neoh KG, Tan KL, Cui CQ, Lim TB. J Adhesion Sci Technol 1997;11:679.

[31] Tan KL, Woon LL, Wong HK, Kang ET, Neoh KG. Macromolecules 1993;26:2832.

[32] Richer J, Stolberg L, Lipkoski J. Langmuir 1986;21:630.

[33] Burrell MC, Codella PJ, Fontana JA, Chera JJ. J Vac Sci Technol 1989;A7:1778.

[34] Young JT, Boerio FJ. Surf Interf Anal 1993;20:341.

[35] Linde H, Gleason RT. J Polym Sci: Part A: Polym Chem 1984;22:3043.

[36] Linde HG. J Polym Sci: Part B: Polym Phys 1988;26:1149.

[37] Gaw K, Kikei M, Kakimoto M, Imai Y. React Funct Polym 1996;30:85.

[38] Gaw K, Kakimoto M. Prog Polyimide Chem I 1999;140:107.